Spine

SPINE Volume 36, Number 26, pp E1666–E1674


ANATOMY

# Psoas Muscle Architectural Design, *In Vivo* Sarcomere Length Range, and Passive Tensile Properties Support Its Role as a Lumbar Spine Stabilizer

Gilad J. Regev, MD,* Choll W. Kim, MD, PhD,*§ Akihito Tomiya, MD, PhD,* Yu Po Lee, MD,* Hossein Ghofrani, MD,* Steven R. Garfin, MD,* Richard L. Lieber, PhD,*† and Samuel R. Ward, PT, PhD*†‡

**Study Design.** Controlled laboratory and cross-sectional study designs.

**Objective.** To determine psoas major (PM) muscle architectural properties, *in vivo* sarcomere-length operating range, and passive mechanical properties.

**Summary of Background Data.** PM is an important hip flexor but its role in lumbar spine function is not fully understood. Several investigators have detailed the gross anatomy of PM, but comprehensive architectural data and *in vivo* length-tension and passive mechanical behaviors have not been documented.

**Methods.** PM was isolated in 13 cadaver specimens, permitting architectural measurements of physiological cross-sectional area (PCSA), normalized fiber length (Lf), and Lf:muscle length (Lm) ratio. Sarcomere lengths were measured *in vivo* from intraoperative biopsies taken with the hip joint in flexed and extended positions. Single-fiber and fiber bundle tensile properties and titin molecular weight were then measured from separate biopsies.

**Results.** Architecturally, average PCSA was 18.45 ± 1.32 $cm^2$, average Lf was 12.70 ± 2 cm, and average Lf:Lm was 0.48 ± 0.06. Intraoperative sarcomere length measurements revealed that the muscle operates from 3.18 ± 0.20 μm with hip flexed at 10.7° ± 13.9° to 3.03 ± 0.22 μm with hip flexed at 55.9° ± 21.4°. Passive mechanical data demonstrated that the elastic modulus of the PM muscle fibers was 37.44 ± 9.11 kPa and of fiber bundles was 55.3 ± 11.8 kPa.

**Conclusion.** Analysis of PM architecture demonstrates that its average $L_f$ and passive biomechanical properties resemble those of the lumbar erector spinae muscles. In addition, PM sarcomere lengths were confined to the descending portion of the length-tension curve allowing the muscle to become stronger as the hip is flexed and the spine assumes a forward leaning posture. These findings suggest that the human PM has architectural and physiologic features that support its role as both a flexor of the hip and a dynamic stabilizer of the lumbar spine.

**Key words:** lumbar spine, muscle architecture, psoas muscle.
**Spine 2011;36:E1666–E1674**

The psoas major (PM) muscle is unique among the paraspinal muscles. It originates both from posterior (transverse process) and anterior (vertebral bodies and intervertebral discs) structures. Along with the iliacus muscle, it inserts into the lesser trochanter of the femur.[1] Although it is widely agreed that the iliopsoas muscle functions as the primary flexor of the hip joint, there is still a debate with regard to its role in the lumbar spine.[2] Assessing the effect of the PM on the lumbar spine is complicated because its fascicles originate from, and span over, multiple moving segments. Furthermore, because of the lumbar lordosis, the muscle segments originating from the upper lumbar segments can function as extensors of the spine in the erect position, whereas the segments that originate from the lower lumbar segments can function as flexors of the spine.[3] Therefore, concerning the biomechanics of the lumbar spine, one is obliged to rely on mathematical or computer modeling techniques to predict muscle forces and moment arms, both of which are difficult or impossible to measure *in vivo*.[2]

The PM has been found to play an important role in various pathologies of the hip and lumbar spine. Atrophy of the PM was observed, both in patients suffering from severe hip joint arthritis and in conditions of spinal degeneration.[4–8] Injury to the iliopsoas tendon has been described in athletes and after total hip arthroplasty.[9,10] Direct injury to the PM

From the *Department of Orthopaedic Surgery, University of California and Veterans Administration Medical Centers, San Diego, CA; †Department of Radiology, University of California, San Diego, CA; ‡Department of Bioengineering, University of California, San Diego, CA; and §Spine Institute of San Diego, Center for Minimally Invasive Spine Surgery at Alvarado Hospital, San Diego, CA.

Acknowledgment date: August 25, 2009. First Revision date: November 1, 2010. Second Revision date: January 23, 2011. Accepted date: March 1, 2011.

The manuscript submitted does not contain information about medical device(s)/drug(s).

No funds were received in support of this work. No benefits in any form have been or will be received from a commercial party related directly or indirectly to the subject of this manuscript.

Address correspondence and reprint requests to Samuel R. Ward, PT, PhD, Department of Radiology, University of California, San Diego, 9500 Gilman Dr (Mail Code 0610), La Jolla, CA 92093; E-mail: srward@ucsd.edu

DOI: 10.1097/BRS.0b013e31821847b3

can also occur during spine surgery when using the minimally invasive, lateral, transpsoas approach.[11] However, the long-term effects of these injuries on the spinal column and the hip joint are unknown.

Because skeletal muscle architecture, defined as the number and orientation of muscle fibers within a muscle, is the only accurate predictor of muscle function.[12,13] High-resolution functional musculoskeletal models rely heavily on architecture to make predictions of muscle function.[14–16] Most studies analyzing the PM architectural properties use either computed tomography[17] or magnetic resonance imaging[18] to estimate muscle cross-sectional area and its location relative to the spine centers of rotation in order to estimate the muscle moment arms in different planes. However, to accurately measure these architectural features, the entire muscle must be studied at the tissue level. Such cross-sectional area calculations from a single image plane are notoriously subject to error because of the fact that muscle fibers themselves rarely traverse precise anatomical planes or run the entire muscle length (Lm).[12,19] Moreover, previous architectural studies have used cadaveric specimens of advanced age.[3,20] Because the PM has been shown to undergo atrophy after the age of 60 years,[21] using data generated from elderly cadaveric specimens may further reduce the accuracy of the data applied to biomechanical models.[22]

Although architectural features of skeletal muscle (*e.g.*, physiological cross-sectional area [PCSA] and fiber length [Lf]) define its maximal force generating capability and excursion, additional information about its functional role can be learned from the physiologic properties of the muscle. For example, it is well established that muscle force generation is length sensitive.[23,24] Therefore, defining the PM sarcomere length–joint angle relationship would determine whether the muscle becomes stronger or weaker as the hip joint flexes. We recently found that the multifidus muscle's sarcomere-length operating range is uniquely confined to the ascending limb of the length-tension curve.[25] However, no analogous sarcomere length joint angle measurements have been reported for any other paraspinal muscle. In addition, passive tension has been shown to be an important component of muscle function, particularly in the lumbar spine.[26] However, the passive tension characteristics of most human muscles remain undefined.

The purpose of this study was to combine quantitative anatomical studies with patient-based intraoperative sarcomere length measurements and passive mechanical analyses to understand the functional capacity and architectural design of the PM muscle. Knowing that the hip is a relatively mobile joint, we hypothesized that because the PM is primarily a flexor of the hip, it would operate over a relatively wide sarcomere-length range and have a relatively low passive elastic modulus, similar to other appendicular muscles.

## MATERIALS AND METHODS

### Architectural Analysis

Thirteen cadaveric specimens, mean age 50 ± 6 years, were used to determine the PM architectural properties (Table 1).

**TABLE 1. Cadaveric Specimen**

| | No. | Age (yr) | Mass (g) | Muscle Length (cm) | Normalized Muscle Length (cm) | Fiber Length (cm) | Normalized Fiber Length (cm) | Sarcomere Length (μm) | PCSA (cm²) |
|---|---|---|---|---|---|---|---|---|---|
| Women | 7 | 53.00 ± 2.5 | 194.08 ± 19.9* | 27.42 ± 2.1 | 24.85 ± 1.3 | 13.17 ± 1.4 | 11.90 ± 1.6 | 3.01 ± 0.3 | 15.51 ± 4.7* |
| Men | 7 | 47.14 ± 6.5 | 304.45 ± 81.6* | 31.96 ± 4.1 | 28.90 ± 5.8 | 14.73 ± 1.7 | 13.22 ± 2.2 | 3.03 ± 0.3 | 21.68 ± 11.7* |
| Combined | 13 | 49.69 ± 5.7 | 249.79 ± 66.4 | 29.93 ± 4 | 27.05 ± 5.2 | 14.11 ± 1.7 | 12.69 ± 2.0 | 3.03 ± 0.3 | 18.45 ± 4.7 |
| Friederich *et al*[22] | 2 | 50 | … | 24.8 | … | 11.3 ± 0.29 | … | … | 14.73 |
| Ward *et al*[20] | 19 | 82.52 ± 9.42 | 195.37 ± 7.7 | 27.42 ± 2.99 | 24.85 ± 2.7 | 13.34 ± 1.39 | 11.69 ± 1.26 | 3.11 ± 0.28 | 12.04 ± 4.61 |

**Significantly different ($P < 0.05$) between men and women.*

*PCSA indicates physiological cross-sectional area.*

| TABLE 2. Patient Biopsy Data | | |
|---|---|---|
| Characteristic | *In Vivo* Sarcomere Length Study | Passive Mechanics Study |
| Age (yr) | 70 ± 7 | 69 ± 11 |
| Patients (no.) | 10 | 9 |
| Sex | 2 M and 8 F | 1 M and 8 F |
| Biopsy level | | |
| L1–L2 | 0 | 1 |
| L2–L3 | 1 | 0 |
| L3–L4 | 1 | 0 |
| L4–L5 | 8 | 8 |

Muscle architecture was determined according to the methods of Sacks and Roy[27] and as previously described in detail by Ward *et al*[20] for muscles of the human lower extremity. Briefly, the PM muscles from formalin-fixed cadavers were harvested *en bloc* and stripped of superficial connective tissue. The external portions of the tendon of the muscles were removed. Muscle length (Lm) was defined as the distance from the origin of the most proximal fibers to the insertion of the most distal fibers. Surface pennation angle was measured as the orientation of the fibers in each of 3 predefined regions relative to the line of action of the distal tendon. Fiber bundle length was measured using a digital caliper (accuracy, 0.01 mm). To compensate for variations in raw Lf that occur because of the position of the spine and hip during fixation, muscle Lfs were normalized by measuring sarcomere length and then scaling the raw Lf to an optimal sarcomere length in human muscle of 2.7 μm.[28] This approach allowed for direct comparison of Lfs from different PM regions and among other spine and lower extremity muscles.

In addition to the above measurements, the following parameters were calculated: $L_f$:$L_m$ ratio and PCSA according to the following previously-validated equation:[12]

$$PCSA\,(cm^2) = \frac{M(g) \times \cos\theta}{\rho\,(g/cm^3) \times L_f\,(cm)}$$

where θ is pennation angle and ρ is muscle density (1.112 g/cm$^3$).[29] The $L_f$:$L_m$ ratio is an index of the excursion design. For example, muscles that contain fibers that span the entire $L_m$ ($L_f$:$L_m$ ratio = 1.0) are designed more for excursion than the muscles that have fibers spanning half of the $L_m$ ($L_f$:$L_m$ ratio = 0.5). This ratio is a useful parameter to consider because it is independent of the absolute magnitude of muscle $L_f$ and muscle size. PCSA was calculated because it is the only muscle structural parameter known to accurately predict the maximum force produced by a muscle.[12] The accuracy and precision of these measurements have been previously reported[20,30] and their relationships to muscle performance have been well documented.[31,32]

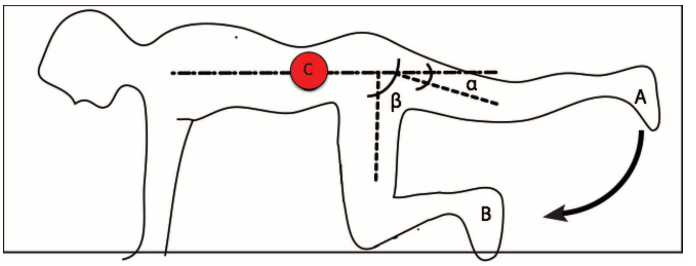


**Figure 1.** Schematic illustration demonstrating patient position during intraoperative psoas major biopsy. The patient's hip is positioned in extension (**A**) during the first biopsy and then flexed at the hip joint for the second biopsy (**B**). Hip flexion angles are measured accordingly (α, β) before each biopsy. Location of psoas major biopsy (**C**).

## *In Vivo* Sarcomere Length

Under a University of California San Diego Human Subjects Protection Program–approved protocol, PM specimens were obtained from patients undergoing lumbar interbody fusion, through a minimally invasive lateral approach (n = 10; Table 2). Patients were positioned on the operating table in the lateral decubitus position with the upper hip joint extended. Using either the XLIF (NuVasive, Inc., San Diego, CA) or DLIF (Medtronic Sofamor Danek Inc., Memphis, TN) techniques, the PM was exposed but not penetrated.[11] A small segment of the PM was isolated by blunt dissection along natural fascicular planes with a long Penfield probe. A specialized clamp[33] was then slipped over the bundle with care to avoid undue manipulation or tension on the muscle (Figure 1). The clamp was deployed and the biopsy of muscle within the jaws of the clamp was resected and immediately placed in formalin to fix the biopsy in its *in vivo* configuration. After flexion of the hip, a second biopsy from a different muscle fascicle was obtained in the same fashion. A large goniometer was used to measure hip joint angle before each biopsy (Figures 2, 3). Laser diffraction was then used to measure the *in vivo* sarcomere lengths.[28,34]

## Passive Single-Fiber and Fiber Bundle Mechanics

A second set of biopsies from a different group of patients (n = 9; Table 2) was obtained to determine PM tensile

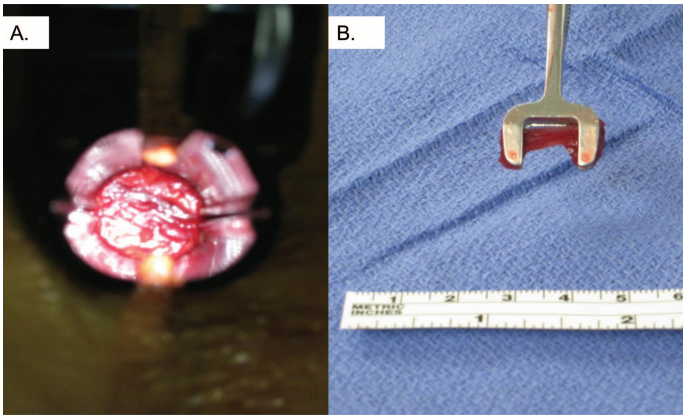


**Figure 2.** Intraoperative pictures taken during psoas major biopsy. **A,** Psoas muscle shown through the MIS retractor blades. **B,** The muscle biopsy can be seen inside the specialized clamp.

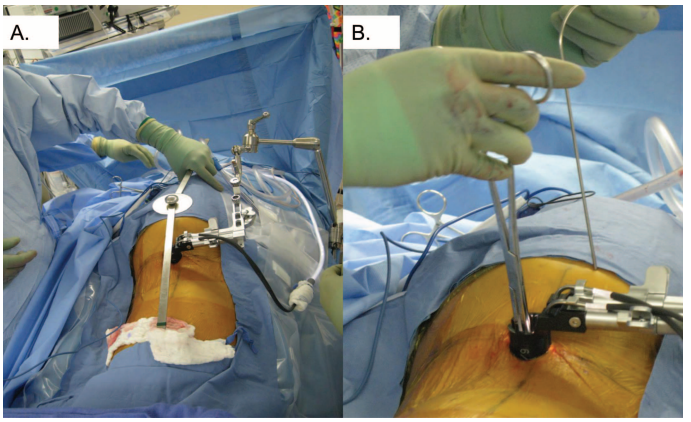


**Figure 3.** Intraoperative pictures taken during psoas major biopsy. **A,** Measurement of hip flexion angle with a goniometer that is placed on the patient. **B,** Biopsy viewed through the MIS surgical retractor within the specialized clamp.

properties. Using the same minimally invasive surgery (MIS) lateral approach described above, a small muscle biopsy was harvested from the muscle. The single-fiber and fiber bundle testing protocol was designed to measure elastic material properties apart from any velocity-dependent properties, as previously described.[35] Briefly, the dissected fiber or fiber bundle segment was secured on either side to 125-μm titanium wires using 10-0 silk suture loops. One wire was secured to an ultrasensitive force transducer (Model 405, sensitivity 10 V/g; Aurora Scientific, Ontario, Canada) and the other was secured to a micromanipulator. The sample was transilluminated by a 7-mW He-Ne laser to permit sarcomere length measurement by laser diffraction.[36] Resolution of this method is approximately 5 nm.[37] The system was calibrated with a 2.50-μm plastic-blazed diffraction grating before experimentation (Diffraction Gratings, Inc., Nashville, TN). After calibration and mounting, samples were lengthened until force registered on a load cell that defined baseline load and slack sarcomere length. To define elastic modulus, mounted samples were lengthened in 250-μm increments after which stress-relaxation was permitted for 2 minutes and both sarcomere length and tension were again recorded. Segments were elongated through the theoretical limit of actin and myosin overlap in human muscle.[28] The slope of the stress-strain curve between 2.0 and 4.25 μm was defined as the elastic modulus. Samples were discarded if they did not produce a clear diffraction pattern, if any irregularities appeared along their length, or if they were severed or slipped at either suture attachment point during testing.

## Analysis of Titin Isoforms

A second muscle biopsy was placed in a microfuge tube and suspended in 50 μL, of sodium dodecyl sulfate (SDS) sample buffer. The samples were stored at −80°C until analyzed by gel electrophoresis. SDS sample buffer was composed of 8 M urea, 2 M thiourea, 3% SDS w/v, 75 mM dithiothreitol, 0.03% bromophenol blue, and 0.05 M Tris-Cl, pH 6.8.[38]

The molecular weight of titin in single fibers was determined using SDS vertical agarose gel electrophoresis, which has been described previously.[38] An acrylamide plug was placed at the bottom of the gel to hold the agarose in place. The final composition of this plug was 12.8% acrylamide, 10% v/v glycerol, 0.5 M Tris-Cl, 2.34% N,N′-diallyltartardiamide, 0.028% ammonium persulfate, and 0.152% N,N,N′,N′-tetramethylethylenediamine. The composition of the agarose gel was 1% w/v Sea Kem Gold agarose (Lonza, Basel, Switzerland), 30% v/v glycerol, 50 mM Tris-base, 0.384 M glycine, and 0.1% w/v SDS. This solution was poured above the acrylamide plug while being warmed to prevent premature solidification.

Titin standards were obtained from human soleus and rat cardiac muscles, which have known molecular weights of approximately 3700 kDa and 2992 kDa, respectively.[39] These tissues were homogenized and stored at -80°C until use. Before loading on the gel, standards were diluted by placing 4-μL human soleus standard and 8-μL rat cardiac standard into 98 μL of sample buffer.

Single-fiber sample tubes were then placed in boiling water for 3 minutes. After cooling, each sample was diluted by adding 5 μL of sample with 4.2 μL of sample buffer and 0.8 μL of rat cardiac titin. Each well was loaded with 10 μL of either standard or sample. The standard cocktail was loaded into every fourth well to permit accurate gel quantification even if the gels distorted slightly. Gels were run at 4°C for 5 hours at 15 mA constant current. Agarose gels were fixed and stained according to the Silver Stain Plus procedure (Sigma-Aldrich Corp., St. Louis, MO) except that gels were dried for approximately 20 hours at 40°C immediately after fixing. Relative mobility and intensity of each band was quantified using a GS-800 Calibrated Densitometer (Bio-Rad, Hercules, CA) and Quantity One 1-D Analysis Software (Bio-Rad). The relative mobility of proteins on the gel was linearly related to the log of their molecular weights. The average correlation coefficient for the gel was determined from the 3 standard lanes containing human soleus titin and rat cardiac titin. Relative mobilities of the unknown PM titins were then based on the distance of those bands from the rat cardiac titin in each lane.

## Data Analysis

Whole-muscle comparisons between PM and the other lumbar spine muscles were made with independent sample *t* tests using the means, standard deviations, and sample sizes reported by Delp *et al*[40] and Ward *et al*.[20,25] The architectural data were modified to represent the muscles' bilateral dimensions, as both parts of the muscle operate on the lumbar spine.[3,20] After screening data for normality and homogeneity of variances, regional comparisons within the muscle were made using one-way analyses of variance with repeated measures. *In vivo* sarcomere lengths are reported for both extended and flexed hip joint positions on a graphical representation of the human sarcomere length-tension curve.[28] For passive mechanical testing, fiber diameter, slack sarcomere length, failure sarcomere length, and elastic modulus were determined. Modulus was defined by the slope of a least squares fit of the stress-strain

curve between sarcomere lengths of 2.0 and 4.25 μm, which represents the physiologic upper limit of actin and myosin filament overlap in humans. Between-muscle comparisons of fiber diameter, fiber bundle diameters, elastic modulus, sarcomere slack length, and titin molecular weight were made using one-way analyses of variance.

To provide context for the modulus value, these data were compared to previously published vastus lateralis[41] and paraspinal muscles.[26] All values are reported as mean ± standard deviation unless otherwise noted. Statistical tests were made using SPSS (version 16.0; SPSS, Inc., Chicago, IL) with *P* values set to 0.05 except for *post hoc* tests where the experiment-wise *P* value of 0.05 was adjusted according to the Sidak correction for multiple comparisons.

## RESULTS

### Muscle Mass

The mass of the PM (249.79 ± 66.43 g) was significantly larger than the other lumbar spine muscles: multifidus (146.1 ± 8.7 g), longissimus thoracis (146.8 ± 13.9 g), iliocostalis lumborum (121.8 ± 13.4 g), or quadratus lumborum (41.2 ± 1.7 g).[25,40] PM mass was not significantly greater in our specimen group (average age = 50 ± 6 years) than in our previously published data (195.37 ± 7.7 g) from older specimens (average age = 83 ± 9 years).[20]

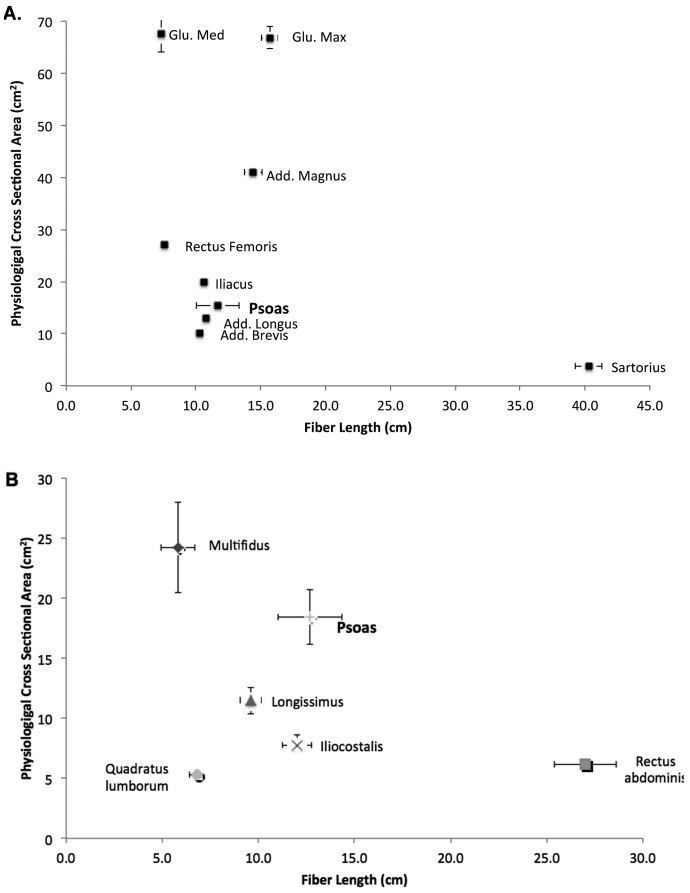


**Figure 4.** Scatter plot of physiological cross-sectional area (PCSA) *versus* fiber length (PCSA values represent the summed right and left side muscles) of the psoas major and the hip muscles (**A**) and the paraspinal muscles (**B**). Since PCSA is proportional to muscle force and fiber length is proportional to muscle excursion, this plot illustrates the muscle's functional design. (Data from muscles other than the psoas major were adapted from Delp *et al*[40] and Ward *et al*[20,25]).

### $L_f$ and PCSA

PM $L_f$ (12.69 ± 2.0 cm) was consistent within different regions of the muscle (coefficient of variation = 11.5%) and, on average, was similar to the $L_f$ s of the erector spinae muscles. However, they were significantly longer than the multifidus muscle (5.66 ± 0.65 cm; Figure 4A). PCSA (18.45 ± 4.7 $cm^2$) was similar to previously published data in older specimens.[3,20] However, PM PCSA was significantly larger than those of the longissimus (11.8 ± 2.5 $cm^2$) and iliocostalis (8.2 ± 1.9 $cm^2$) muscles but significantly smaller than that of the multifidus muscle (23.9 ± 3.0 $cm^2$). Interestingly, PM PCSA was very close to that of the combined lumbar erector spinae muscles (longissimus and iliocostalis, 19.26 ± 2.5 $cm^2$). When comparing PM architectural properties to other muscles that operate over the hip joint (Figure 4B), it was similar in PCSA and $L_f$ to the iliacus, adductor longus, and adductor brevis. However, it had a significantly smaller PCSA than those of the gluteus medius and gluteus maximus.

### *In Vivo* Sarcomere Length

For the *in vivo* clamped muscle biopsy specimens, PM sarcomere length ranged from 3.18 ± 0.3 μm, with the hip joint near extension (10.7° ± 14°) to 3.03 ± 0.22 μm with the hip joint flexed (55.9° ± 21.4°). When the hip joint was flexed, thereby shortening the muscle, sarcomere length shortened significantly ($P < 0.05$). Therefore, throughout the range of motion that could be achieved intraoperatively, the muscle operated exclusively on the descending portion of the length-tension curve (Figure 5). Given that sarcomere lengths cannot be accurately measured in passive muscle when the muscle is very short, we used a simple linear regression model to estimate sarcomere length at hip joint angles greater than 55°. According to our model the PM sarcomeres shorten by 0.04 μm per 1° of hip flexion, which means the muscle would reach a sarcomere length of 2.76 μm (optimal length) at 120° of flexion (Figure 6).

### PM Passive Mechanics

PM single-fiber diameter (70 ± 10 μm) was significantly smaller than previously published data on the multifidus, longissimus, and iliocostalis muscles.[26] Fiber bundle diameter (240 ± 90 μm) was similar to these same muscles. Single-fiber and fiber bundle elastic moduli (37.44 ± 9.11 kPa and 55.33 ± 11.83 kPa, respectively) were similar to other paraspinal muscles, with the exception of multifidus, which had a larger fiber bundle modulus than any other muscle ($P < 0.05$) (Figure 7A, B). PM titin molecular weight (3605 ± 18.6 kDa) was higher than the rest of the paraspinal muscles ($P < 0.05$) (Figure 7C). Thus the PM was found to have a smaller fiber diameter and higher titin isoform molecular weight. However, its fiber elastic modulus was similar to the rest of the paraspinal muscles.[26,41,42] The PM fiber bundle elastic modulus

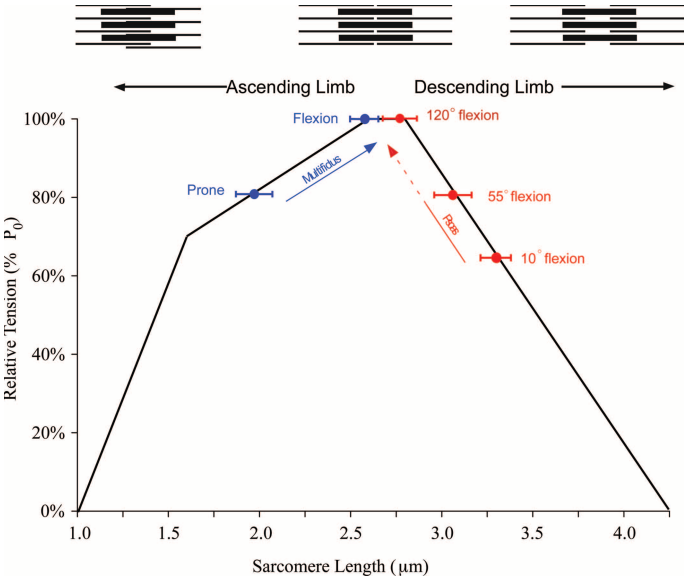


**Figure 5.** Sarcomere length operating range of multifidus and psoas major plotted on the human skeletal muscle sarcomere length-tension curve. These data demonstrate that the psoas major and multifidus muscles operate on the opposite limbs of the length-tension curve. However, both become intrinsically stronger as the spine flexes (arrow). Schematic sarcomeres are shown on the ascending and descending limbs to scale, based on the quantification of actin and myosin filaments lengths reported previously (Lieber et al).[28]

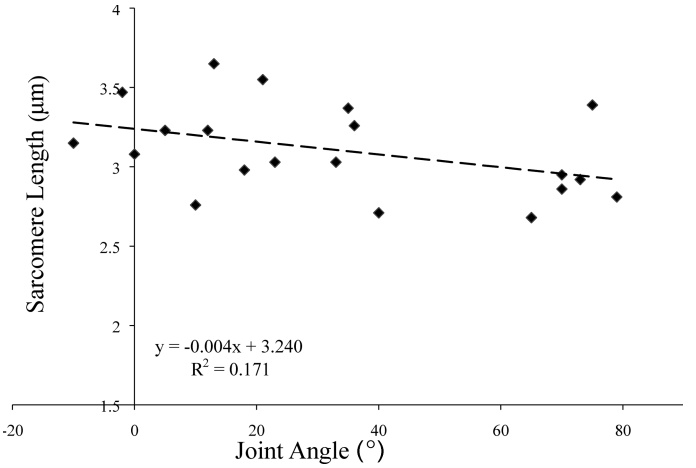


**Figure 6.** Scatter plot of *in vivo* sarcomere length *versus* hip flexion angle. Using a statistical regression model, the estimated moment arm produced by the psoas major over the hip joint as a function of hip joint angle at 55° to 120° of flexion was formulated (dashed line).

was similar to the longissimus and iliocostalis muscles but significantly smaller than the multifidus (Figure 7B).[26]

## DISCUSSION

The objectives of this study were to study the PM architectural characteristics, *in vivo* sarcomere lengths across the hip joint range of motion, and its passive biomechanical properties. The data presented in this study coupled with electrophysiological studies, which analyze movement patterns, can provide us with a better understanding of the PM function in the hip joint and the lumbar spine.

Anatomy textbooks provide us with a superficial description of the PM function as a forward and lateral flexor of the lumbar spine on the basis of its origin and insertion. However, there is still a debate in the literature regarding its ability to function as a stabilizer of the lumbar spine, Bogduk *et al*[3] argued, on the basis of the PM lines of action and moment arms, that the muscle produces large shear forces in the lumbar spine and therefore suggested that it can not act as a stabilizer of the lumbar spine. However, this theory was contradicted by Santaguida *et al*,[18] who argued that Bogduk *et al* mistakenly overestimated the shear forces and underestimated the stabilizing compression produced by the PM over the lumbar spine, leaving the question unresolved.

In terms of physiology, our findings support the hypothesis that the PM is not designed solely as a hip flexor. Although PM PCSA, Lf, and tensile properties are comparable to other muscles that cross the hip joint,[20,26] its sarcomere-length operating range is uniquely confined to the descending region of the length-tension curve.[43] This demonstrates that the PM is not designed to produce its maximal forces during walking or running but rather in positions of high hip flexion, such as in forward bending or sitting.

Furthermore, data presented in this study suggest that with regard to its PCSA, Lf, and passive tensile properties, architecturally the PM also closely resembles other erector spinae muscles. This finding indicates that these muscle groups, arising from opposites sides of the spine may be designed to operate as antagonists. The similarity in force-generating capacity between these 2 muscle groups is interesting because it demonstrates the fact that PM forces acting on the lumbar spine are different than those produced at its hip insertion, where its distal tendon conjoins the iliacus muscle. Electrophysiological studies suggested that among trunk muscles, cocontraction of antagonistic muscles stabilizes the lumbar spine by producing compression forces along the spine axis.[44,45] Therefore, similarity in architectural design of antagonistic muscle groups within the lumbar spine supports a synergistic function of these muscles over the lumbar spine.

As further support for these muscles acting as functional antagonists, we found that the PM and the posterior paraspinal muscles operate on opposite sides of the sarcomere length-tension curve. It has been demonstrated that wrist flexors and extensors operate on opposite sides of the sarcomere length-tension curve, and have similar elastic moduli, which creates a precise mechanical balance between flexion and extension moments throughout the range of wrist motion.[28] The sarcomere length-tension relationship is one of the classic structure-function relationships in biology. The anatomical basis of this relationship is the changing interdigitation of actin and myosin filaments with changing sarcomere length. Thus, as the hip joint and the spine flex, sarcomere length decreases and muscle force increases, whereas with the spine erect and the hip joint extended, sarcomere length increases and muscle force decreases.

This finding suggests a synergistic protective function of PM and posterior paraspinal muscles over the lumbar spine,

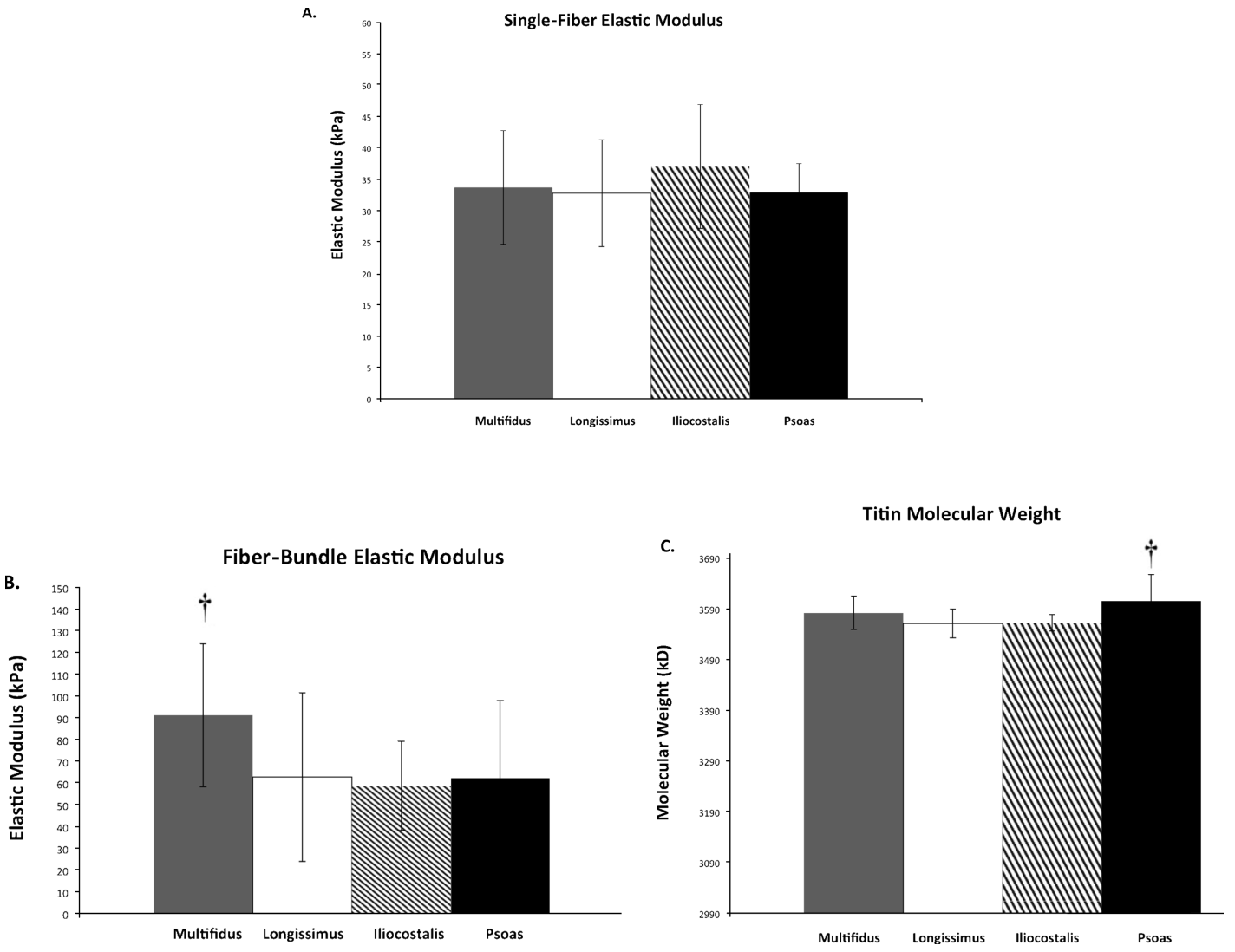


**Figure 7.** Comparison of single-fiber elastic modulus (**A**), fiber bundle elastic modulus (**B**), and titin molecular weight (**C**) in psoas major (PM), longissimus, iliocostalis, and multifidus muscles. Moduli were calculated as the slopes of the stress-strain curves in the sarcomere length range of 2.0 to 4.25 μm. * indicates significant differences between PM and multifidus. Data are presented as mean ± SD. (Data from muscles other than PM were obtained from Ward *et al*[26]).

because both muscle groups become intrinsically stronger as the spine flexes forward. This design is especially appealing as it creates a proportional feedback system in which the greater the deflection from the neutral zone, the greater the restoring force. This provides the necessary stabilizing force as the body leans forward, a position known to elevate intradiscal pressure and perhaps lead to increased low back pain in patients with spinal disorders.[46,47] Clinically, this finding may help explain the ability of the PM to produce forces over the spine with different exercises that are routinely prescribed during rehabilitation of low back pain patients. As an example, opposite to common belief, during knee-bent sit-up exercise the PM ability to generate forces over the lumbar spine increases compared with straight hips/legs sit-ups.

The results of this study have specific applications to spine clinical practice as they suggest that the function of the PM as a spine stabilizer must be acknowledged. Although we did not explicitly measure PM function, the high-resolution PCSA, Lf, and sarcomere operating length measurements strongly suggest that the effects of injury to the muscle or to its tendinous attachment to the lesser trochanter on the femur, might not simply be limited to reduction in hip flexion force.[48,49] Although, we are not aware of studies that analyzed the effect of PM injury on spinal stability, clinical studies have found a higher incidence of unilateral psoas muscle atrophy and back pain after proximal femoral fractures.[50,51] Similarly, unilateral psoas and multifidus atrophy was observed in patients with chronic low back pain.[7]

There are several potential confounding factors that need to be recognized when discussing our findings, as well as, previously published anatomic and morphometric studies. First, the cadaveric specimens were obtained from a small and heterogenic group of cadavers whose cause of death and medical history were unknown to us, making it difficult to assess their health and activity levels before death. These factors may explain the surprising similarity in PM mass and PCSA

as with previously published data that were obtained from a much older participant group. Second, patients from whom the muscle biopsies were taken might not have had a normal, healthy PM because they suffered from degenerative spine conditions, which might cause their PM to become relatively atrophic. Last, we acknowledge that multiple factors may contribute to *in vivo* PM function, such as agonist and antagonist recruitment patterns and the combined three-dimensional positions of the hip and spine. Future studies are needed to further elucidate the complex structures and interaction of the paraspinal muscles as well as to fully comprehend their function during spinal movement and perturbation.

## ➢ Key Points

- ❑ PM had intermediate Lfs and PCSA compared with other lumbar spine and hip muscles, allowing it to generate moderate forces over a wide range of lengths.
- ❑ The passive mechanical properties of PM muscle fibers were similar to the paraspinal muscles but significantly less stiff than the multifidus muscle.
- ❑ *In vivo* sarcomere lengths during hip flexion were confined to the descending portion of the length-tension curve, allowing the muscle to become stronger as the hip is flexed and the spine assumes a forward leaning posture.
- ❑ These findings suggest that the human PM has architectural and physiologic features that support its role as both a flexor of the hip and as a dynamic stabilizer of the lumbar spine.

## References


1. Warwick R, Williams PL. *Gray's Anatomy*. 35th ed. London, United Kingdom: Longman; 1973.
2. Hansen L, de Zee M, Rasmussen J, et al. Anatomy and biomechanics of the back muscles in the lumbar spine with reference to biomechanical modeling. *Spine* 2006;31:1888–99.
3. Bogduk NM, Pearcy M, Hadfield G. Anatomy and biomechanics of psoas major. *Clin Biomech* 1992;7:109–19.
4. Rasch A, Bystrom AH, Dalen N, et al. Reduced muscle radiological density, cross-sectional area, and strength of major hip and knee muscles in 22 patients with hip osteoarthritis. *Acta Orthop* 2007;78:505–10.
5. Rasch A, Bystrom AH, Dalen N, et al. Persisting muscle atrophy two years after replacement of the hip. *J Bone Joint Surg Br* 2009;91:583–8.
6. Hides JA, Belavy DL, Stanton W, et al. Magnetic resonance imaging assessment of trunk muscles during prolonged bed rest. *Spine* 2007;32:1687–92.
7. Barker KL, Shamley DR, Jackson D. Changes in the cross-sectional area of multifidus and psoas in patients with unilateral back pain: the relationship to pain and disability. *Spine* 2004;29:E515–19.
8. Mayer TG, Vanharanta H, Gatchel RJ, et al. Comparison of CT scan muscle measurements and isokinetic trunk strength in postoperative patients. *Spine* 1989;14:33–6.
9. Bui KL, Ilaslan H, Recht M, et al. Iliopsoas injury: an MRI study of patterns and prevalence correlated with clinical findings. *Skeletal Radiol* 2008;37:245–9.
10. Dora C, Houweling M, Koch P, et al. Iliopsoas impingement after total hip replacement: the results of non-operative management, tenotomy, or acetabular revision. *J Bone Joint Surg Br* 2007;89:1031–5.
11. Ozgur BM, Aryan HE, Pimenta L, et al. Extreme lateral interbody fusion (XLIF): a novel surgical technique for anterior lumbar interbody fusion. *Spine J* 2006;6:435–43.
12. Powell PL, Roy RR, Kanim P, et al. Predictability of skeletal muscle tension from architectural determinations in guinea pig hindlimbs. *J Appl Physiol* 1984;57:1715–21.
13. Lieber RL, Friden J. Clinical significance of skeletal muscle architecture. *Clin Orthop Relat Res* 2001;383:140–51.
14. Delp SL, Loan JP, Hoy MG, et al. An interactive graphics-based model of the lower extremity to study orthopaedic surgical procedures. *IEEE Trans Biomed Eng* 1990;37:757–67.
15. Macintosh JE, Pearcy MJ, Bogduk N. The axial torque of the lumbar back muscles: torsion strength of the back muscles. *Aust N Z J Surg* 1993;63:205–12.
16. Stokes IA, Gardner-Morse M. Quantitative anatomy of the lumbar musculature. *J Biomech* 1999;32:311–6.
17. Dumas GA, Poulin MJ, Roy B, et al. Orientation and moment arms of some trunk muscles. *Spine* 1991;16:293–303.
18. Santaguida PL, McGill SM. The psoas major muscle: a three-dimensional geometric study. *J Biomech* 1995;28:339–45.
19. Gatton ML, Pearcy MJ, Pettet GJ. Difficulties in estimating muscle forces from muscle cross-sectional area. An example using the psoas major muscle. *Spine* 1999;24:1487–93.
20. Ward SR, Eng CM, Smallwood LH, et al. Are current measurements of lower extremity muscle architecture accurate? *Clin Orthop Relat Res* 2009;467:1074–82.
21. Takahashi K, Takahashi HE, Nakadaira H, et al. Different changes of quantity due to aging in the psoas major and quadriceps femoris muscles in women. *J Musculoskelet Neuronal Interact* 2006;6:201–5.
22. McGill SM, Patt N, Norman RW. Measurement of the trunk musculature of active males using CT scan radiography: implications for force and moment generating capacity about the L4/L5 joint. *J Biomech* 1988;21:329–41.
23. Gordon AM, Huxley AF, Julian FJ. The variation in isometric tension with sarcomere length in vertebrate muscle fibres. *J Physiol* 1966;184:170–92.
24. Gordon AM, Huxley AF, Julian FJ. Tension development in highly stretched vertebrate muscle fibres. *J Physiol* 1966;184:143–69.
25. Ward SR, Kim CW, Eng CM, et al. Architectural analysis and intraoperative measurements demonstrate the unique design of the multifidus muscle for lumbar spine stability. *J Bone Joint Surg Am* 2009;91:176–85.
26. Ward SR, Tomiya A, Regev GJ, et al. The passive mechanical properties of the lumbar multifidus support its role as a stabilizing muscle. *J Biomech* 2009;42:1384–9.
27. Sacks RD, Roy RR. Architecture of the hindlimb muscles of cats: functional significance. *J Morphol* 1982;173:185–95.
28. Lieber RL, Loren GJ, Frid J. *In vivo* measurement of human wrist extensor muscle sarcomere length changes. *J Neurophysiol* 1994;71:874–81.
29. Ward SR, Lieber RL. Density and hydration of fresh and fixed skeletal muscle. *J Biomech* 2005;38:2317–20.
30. Takahashi M, Ward SR, Lieber RL. Intraoperative single-site sarcomere length measurement accurately reflects whole-muscle sarcomere length in the rabbit. *J Hand Surg Am* 2007;32:612–17.
31. Winters TM, Takahashi M, Lieber RL, et al. Whole muscle length-tension relationships are accurately modeled as scaled sarcomeres in rabbit hindlimb muscles. *J Biomech* 2011;44:109–15.
32. Powell PL, Roy RR, Kanim P, et al. Predictability of skeletal muscle tension from architectural determinations in guinea pig hindlimbs. *J Appl Physiol* 1984;57:1715–21.
33. Ward SR, Takahashi M, Winters TM, et al. A novel muscle biopsy clamp yields accurate *in vivo* sarcomere length values. *J Biomech* 2009;42:193–6.
34. Lieber RL, Fazeli BM, Botte MJ. Architecture of selected wrist flexor and extensor muscles. *J Hand Surg Am* 1990;15:244–50.
35. Fung YC. *Biomechanics: Mechanical Properties of Living Tissues*. New York, NY: Springer Verlag; 1981.
36. Lieber RL, Yeh Y, Baskin RJ. Sarcomere length determination using laser diffraction. Effect of beam and fiber diameter. *Biophys J* 1984;45:1007–16.

37. Baskin RJ, Roos KP, Yeh Y. Light diffraction study of single skeletal muscle fibers. *Biophys J* 1979;28:45–64.
38. Warren CM, Krzesinski PR, Greaser ML. Vertical agarose gel electrophoresis and electroblotting of high-molecular-weight proteins. *Electrophoresis* 2003;24:1695–702.
39. Freiburg A, Trombitas K, Hell W, et al. Series of exon-skipping events in the elastic spring region of titin as the structural basis for myofibrillar elastic diversity. *Circ Res* 2000;86:1114–21.
40. Delp SL, Suryanarayanan S, Murray WM, et al. Architecture of the rectus abdominis, quadratus lumborum, and erector spinae. *J Biomech* 2001;34:371–5.
41. Boakes JL, Foran J, Ward SR, et al. Muscle adaptation by serial sarcomere addition 1 year after femoral lengthening. *Clin Orthop Relat Res* 2007;456:250–3.
42. Fridén J, Lieber RL. Spastic muscle cells are shorter and stiffer than normal cells. *Muscle Nerve* 2003;27:157–64.
43. Burkholder TJ, Lieber RL. Sarcomere length operating range of vertebrate muscles during movement. *J Exp Biol* 2001;204:1529–36.
44. Granata KP, Marras WS. Cost-benefit of muscle cocontraction in protecting against spinal instability. *Spine* 2000;25:1398–404.
45. Kavcic N, Grenier S, McGill SM. Determining the stabilizing role of individual torso muscles during rehabilitation exercises. *Spine* 2004;29:1254–65.
46. Andersson GB, Ortengren R, Nachemson A. Intradiskal pressure, intra-abdominal pressure, and myoelectric back muscle activity related to posture and loading. *Clin Orthop Relat Res* 1977;129:156–64.
47. Snook SH, Webster BS, McGorry RW, et al. The reduction of chronic nonspecific low back pain through the control of early morning lumbar flexion. A randomized controlled trial. *Spine* 1998;23:2601–7.
48. Delp SL, Maloney W. Effects of hip center location on the moment-generating capacity of the muscles. *J Biomech* 1993;26:485–99.
49. Delp SL, Zajac FE. Force- and moment-generating capacity of lower-extremity muscles before and after tendon lengthening. *Clin Orthop Relat Res* 1992:247–59.
50. DiLorenzo L, Forte A, Formisano R, et al. Low back pain after unstable extracapsular hip fractures: randomized control trial on a specific training. *Eura Medicophys* 2007;43:349–57.
51. DiLorenzo L, Forte A, Landolfi A, et al. Chronic lumbago after unstable intertrochanteric femoral fracture: a new syndrome or sporadic feature of hip biomechanics after surgery? A case report [in Italian]. *G Ital Med Lav Ergon* 2007;29:210–3.
52. Friederich JA, Brand RA. Muscle fiber architecture in the human lower limb. *J Biomech* 1990;23:91–5.